

Revisiting the solar tachocline: Average properties and temporal variations

H. M. Antia

Tata Institute of Fundamental Research, Homi Bhabha Road, Mumbai 400005, India

`antia@tifr.res.in`

and

Sarbani Basu

Department of Astronomy, Yale University, P. O. Box 208101, New Haven CT 06520-8101, U.S.A.

`sarbani.basu@yale.edu`

ABSTRACT

The tachocline is believed to be the region where the solar dynamo operates. With over a solar cycle's worth of data available from the MDI and GONG instruments, we are in a position to investigate not merely the average structure of the solar tachocline, but also its time variations. We determine the properties of the tachocline as a function of time by fitting a two-dimensional model that takes latitudinal variations of the tachocline properties into account. We confirm that if we consider central position of the tachocline, it is prolate. Our results show that the tachocline is thicker at higher latitudes than the equator, making the overall shape of the tachocline more complex. Of the tachocline properties examined, the transition of the rotation rate across the tachocline, and to some extent the position of the tachocline, show some temporal variations.

Subject headings: Sun: Helioseismology; Sun: Rotation; Sun: Activity; Sun: Interior

1. Introduction

Inversions of helioseismic data have shown that the solar convection zone rotates differentially, but that the radiative interior has an almost solid-body like rotation (see Schou

et al. 1998 and references therein). The transition from differential rotation to solid body rotation occurs over a very narrow region, that is called the tachocline (Spiegel & Zahn 1992). The tachocline is believed to be the seat of the solar dynamo, and hence is expected to affect, and be affected by, the solar dynamo.

The poor resolution of the inversion techniques, particularly at high latitudes, makes it difficult to infer the properties of the tachocline from normal inversions for the solar rotation rate. One consequence of the poor resolution is that the transition appears to occur over a large radial distance. As a result, tachocline studies usually involve forward modelling techniques, with the parameters of the models determined by fitting helioseismic data (e.g., Kosovichev 1996; Basu 1997; Antia et al. 1998; Charbonneau et al. 1999; Basu & Antia 2001, 2003). Early investigations have shown that the tachocline is prolate. Also clear (even from inversions) is that the ‘jump’ in the rotation rate across the tachocline is latitude dependent. At the equator, the rotation rate changes from a higher value to a lower value when moving from the convection zone to the radiative interior through the tachocline, there is almost no change around a latitude of about 30° , while at higher latitudes the rotation rates shifts from a lower value to a higher one. What is not completely clear from earlier work however, is whether the tachocline thickness, i.e., the radial distance over which the rotation rate changes, is larger at higher latitudes than the equator. Although, the early results found that the thickness does increase with latitude, the statistical significance of this increase was not clear.

The bulk of the solar convection zone shows clear, periodic, changes in the rotation rate in the form of zonal flows (Vorontsov et al. 2002; Basu & Antia 2003; Howe et al. 2005). It is, however, not clear if the tachocline too changes with time. Early studies by Basu & Antia (2001; 2003) using data available for a limited part of the solar cycle 23 during its ascending phase did not find any significant temporal variation. However, with more than a solar cycle worth of data available now, we revisit the question of tachocline variations. We also examine whether the tachocline structure was different between the solar minimum preceding cycle 23 and the exceptionally long and deep minimum that preceded cycle 24. We also use the increased amount of data to determine the average properties of the tachocline more accurately.

2. Data and analysis

We use data obtained by the GONG (Hill et al. 1996) and MDI (Schou 1999) projects for this work. These data sets consist of the mean frequency and the splitting coefficients of different (n, ℓ) multiplets. Only the odd-order splitting coefficients are needed to determine

the rotation rate in the solar interior (e.g., Ritzwoller & Lively 1991). We use 151 data sets from GONG, each set covering a period of 108 days. The first set starts on 1995, May 7 and the last set ends on 2010, June 4, with a spacing of 36 days between consecutive data sets. Thus these sets cover about a year of data leading to the minimum of cycle 23 as well as about a year of data following the minimum of cycle 24. The MDI data consist of 73 non-overlapping sets each obtained from observations taken over a period of 72 days. The first set begins on 1996, May 1 and the last set ends on 2011, February 11. The MDI data start close to the minimum of cycle 23 and do not cover preceding period, while these data cover a period of more than a year following the minimum of cycle 24.

To determine the properties of the tachocline we use the 2D-annealing technique described by Antia et al. (1998). In this method we fit a rotation rate of the form

$$\Omega_{\text{tac}}(r, \theta) = \begin{cases} \Omega_c + \frac{\delta\Omega}{1+\exp[(r_t-r)/w]} & \text{if } r \leq 0.70 \\ \Omega_c + B(r - 0.7) + \frac{\delta\Omega}{1+\exp[(r_t-r)/w]} & \text{if } 0.70 < r \leq 0.95 \\ \Omega_c + 0.25B - C(r - 0.95) + \frac{\delta\Omega}{1+\exp[(r_t-r)/w]} & \text{if } r > 0.95 \end{cases} \quad (1)$$

where r is the radial distance in units of solar radius, θ is the co-latitude and

$$B = B_1 + B_3 P_3(\theta) + B_5 P_5(\theta), \quad (2)$$

$$\delta\Omega = \delta\Omega_1 + \delta\Omega_3 P_3(\theta) + \delta\Omega_5 P_5(\theta), \quad (3)$$

$$r_t = r_{d1} + r_{d3} P_3(\theta), \quad (4)$$

$$w = w_1 + w_3 P_3(\theta), \quad (5)$$

$$P_3(\theta) = 5 \cos^2 \theta - 1, \quad (6)$$

$$P_5(\theta) = 21 \cos^4 \theta - 14 \cos^2 \theta + 1. \quad (7)$$

The quantity r_t is the central point of the transition region in the rotation rate and what we consider to be the ‘position’ of the tachocline. The half-width of the tachocline is given by the quantity w , and $\delta\Omega$ is the jump in the rotation rate across the tachocline. The quantities r_t , w and $\delta\Omega$ define the tachocline. The form for the smooth part of rotation rate used here is slightly different from that used by Basu & Antia (2001). The difference is in the radiative interior ($r < 0.7R_\odot$) where we assume uniform rotation. The rotation rate given by Eq. (1) is used to calculate the splitting coefficients and these are compared with observed splitting coefficients. We find that the first component in $\delta\Omega$ is generally small and that the fits become more stable if that is ignored, hence all results in this work are obtained by setting $\delta\Omega_1 = 0$. The parameters $r_{d1}, r_{d3}, w_1, w_3, \delta\Omega_3, \delta\Omega_5, B_1, B_3, B_5, C$, and Ω_c are fitted to the observed splitting coefficients. Only the first 3 odd-order splitting coefficients are used for this purpose. We use the method of simulated annealing to perform the least squares fit to the observed frequencies. Note that our model of the tachocline differs from that of

Kosovichev (1996) and Charbonneau et al. (1999) and to compare the width we obtain to those obtained by them, w needs to be multiplied by a factor of 2.5.

For each available data set in GONG and MDI data sets we fit rotation rate of the form given by Eq. (1) to the observed splitting coefficients to calculate the 11 parameters of the model. In this work we are only interested in the parameters that define the properties of the tachocline.

3. Results and discussion

3.1. The time-averaged tachocline

The time averaged parameters for the tachocline are listed in Table 1. The average tachocline properties were determined by averaging all results. GONG and MDI results were averaged, and are listed, separately. The average results are consistent with those of Basu & Antia (2001) obtained using a subset of current data and with a slightly different form for the rotation rate. As can be seen, that there are some systematic differences between the GONG and MDI results. Similar differences have been seen in rotation inversion results (Schou et al. 2002). The discrepancy is mainly attributed to differences in the data processing pipelines of the two projects. Studies of temporal variations in solar rotation rate (e.g., Antia et al. 2008a) suggest that the time-varying component of the rotation rate is not affected by the discrepancy between GONG and MDI data.

The fitted parameters can be used to calculate the properties of the tachocline at any given latitude. The time-averaged results at a few latitudes are shown in Table 2. As can be seen clearly, the tachocline is prolate as measured by the central radius defining the tachocline. GONG data yields a difference of $(0.012 \pm 0.002)R_{\odot}$ between the latitude of 60° and the equator. The difference with MDI data is $(0.040 \pm 0.003)R_{\odot}$. Our results are in agreement with earlier results (Antia et al. 1998; Corbard et al. 1998, 1999; Charbonneau et al. 1999; Basu & Antia 2001, 2003).

Table 2 also shows a clear variation of the thickness of the tachocline. What we find is that the tachocline is the least thick at the equator, and the thickness increases steadily with latitude. While earlier investigations (Charbonneau et al. 1999; Basu & Antia 2001, 2003) had indicated that this might be the case, the results were not statistically significant. The larger quantity of data available now has resolved this issue. We find that the thickness increases by about $(0.018 \pm 0.003)R_{\odot}$ between the equator and 60° latitude as per GONG and $(0.028 \pm 0.004)R_{\odot}$ as per MDI data.

While the central part of the tachocline (as define by r_t) is clearly prolate in shape, the overall shape of the tachocline is more complex since the thickness changes. Given the model of the tachocline (Eq. 1), we can assume that the tachocline is bounded between layers with radius $r_t - 2w$ and $r_t + 2w$. The rotation rate changed by about 76% of $\delta\Omega$ within these limits. The upper boundary of the tachocline is clearly prolate since both r_t and w increase with latitude. The lower boundary is another matter. Given the tachocline model adopted in this work, the lower boundary is determined by the value of $r_{t3} - 2w_3$, which is $-(0.0071 \pm 0.0021)R_\odot$ (GONG) or $-(0.0066 \pm 0.0030)R_\odot$ (MDI). Thus within 2–3 σ , the lower boundary is close to being spherical. A similar conclusion was reached by Basu & Antia (2003). It should be noted that the base of the convection zone is also spherical (Basu & Antia 2001). The lower boundary of the tachocline is at about $0.68R_\odot$ which is consistent with the extent of mixing required below the solar convection zone to match the solar sound-speed profile (e.g., Brun et al. 2002).

The latitudinal variation in $\delta\Omega$ is very clear. There is very little change in the rotation rate across the tachocline at a latitude of about 30° . At lower latitudes $\delta\Omega$ is positive (i.e., higher rotation rate above the tachocline), while at higher latitudes the sign of the difference is reversed. The latitude at which $\delta\Omega$ changes sign is of some interest. With the parameters of tachocline as determined by us this turns out to be about 29° . If $P_3(\theta)$ were the only term present in the definition of $\delta\Omega$, we would expect this number to be 26.6° . Given that $P_3(\theta)$ is the dominant term, it is not surprising that the latitude at which $\delta\Omega = 0$ is close to this value. The latitude at which $\delta\Omega = 0$ can also be determined quite easily by inspecting solar rotation profiles obtained from inversions. The numbers are quite similar.

3.2. Activity and time dependence

In order to detect tachocline variations linked to solar activity, we also average results that correspond to times of high and low activity — we define the period of high activity to be the one for which the 10.7 cm radio flux was greater than 140 SFU and the period of low activity is defined as the ones with 10.7 cm flux less than 90 SFU. To study possible difference between the two periods of minimum activity covered by the data sets we also take separate averages for the two periods of low activity. These are also listed in Table 1.

We do not find any significant change in either the thickness or the position of the tachocline between the high and low activity periods. However, $\delta\Omega_3$ and $\delta\Omega_5$ show differences at the level of 2–3 σ . To check for any solar cycle variation we also calculate the correlation coefficient between these parameters and the 10.7 cm radio flux. The correlation coefficients for $\delta\Omega_3$ and $\delta\Omega_5$ are found to be 0.40 and 0.20 respectively, when GONG data is used.

For MDI data these correlations are 0.36 and 0.40 respectively. The correlation with other parameters of the tachocline are found to be very small.

GONG and MDI give somewhat disparate results about the differences in the tachocline between the minimum before cycle 23 and that before cycle 24. This could be a result of the fact that MDI data do not completely span the cycle 23 minimum. The only significant change is in the parameter $\delta\Omega_5$. Even that is of opposite sign between GONG and MDI. Thus we cannot say for certain whether the tachocline parameters were different between the two minima.

We take a closer look at the changes in tachocline parameters by examining a few latitudes in more detail. For each latitude we have determined the correlation coefficient between r_t , $\delta\Omega$ and w and the 10.7 cm radio flux. However, since the 10.7 cm flux is an indicator of global activity, while the changes in the tachocline may be correlated with other local changes, which depend on latitude, we also fit an oscillatory form with a period of solar cycle. Thus for $\delta\Omega$ we fit

$$\delta\Omega(t, \theta) = \langle \delta\Omega \rangle + \sum_{k=1}^3 a_k(\theta) \sin(k\omega_0 t + \phi_k) \quad (8)$$

where ω_0 is the frequency corresponding to 11.7 years, the dynamical length of the solar cycle as determined by Antia & Basu (2010), and the angular brackets denote average over time. This form was motivated by the fact that the change of zonal flow velocities at a given latitude and radius can be fitted with this expression. We fit similar expressions to r_t and w .

In Figure 1 we show the position of the tachocline, r_t at four latitudes plotted as a function of time. As can be seen, there is a large spread in the results and there is no clear temporal variation. In the same figure we also show a running mean of the results to reduce the scatter. The running mean is taken over a period of about 1 year, i.e., over 9 sets for GONG and 5 sets for MDI. Also shown is the fit to the form given by Eq. (8). There is a good agreement between the results obtained using GONG and MDI data at low latitudes, but there are significant differences at high latitudes as also seen in the time-averaged data. The r_t values are not correlated with the 10.7 cm flux, the correlation coefficients lie between -0.14 and 0.02 for the different latitudes and sets of data. There appears to be an oscillatory time variation at the lower latitudes, and the results are consistent for both data sets, implying the results may have some significance. Figure 2 shows similar results for the width. At low latitudes the width is comparable to errors in individual data points and it is difficult to say much about the temporal variations. At high latitudes also the temporal variations are unclear — there is no agreement between results obtained with the GONG and MDI data. As with r_t , the correlation with the 10.7 cm flux is small.

Figure 3 shows results for $\delta\Omega$. GONG and MDI results agree at most latitudes, though the agreement is poor at 60° . This is the only quantity that shows a reasonable correlation with the 10.7 cm flux, being correlated with activity at high latitudes and anti-correlated at low latitudes. The correlation coefficient for latitudes 0° , 15° , 45° , and 60° is respectively -0.31 , -0.39 , 0.36 and 0.39 for the GONG data, and -0.22 , -0.34 , 0.20 and 0.41 for MDI. These correlations are consistent with that seen in rotational kinetic energy in the lower part of the convection zone (Antia et al. 2008b) which also shows correlation at high latitude and anti-correlation at low latitudes. Each latitude shows some type of oscillatory behavior in addition to the solar cycle variation, however, the oscillatory behavior of the GONG and MDI results do not agree at any latitude and are out of phase with each other.

Inversion results for rotation rate suggest that the zonal flow pattern penetrates through the convection zone (Vorontsov et al. 2002; Basu & Antia 2003; Howe et al. 2005; Antia et al. 2008a), which could imply some temporal variations in the tachocline region. However, this variation could be in what we consider the smooth part of the rotation rate (parameters Ω_c , B and C in Eq. 1) and may not necessarily affect the tachocline properties r_t , w or $\delta\Omega$. The temporal variation that we find in $\delta\Omega$ is indeed of the same order as the temporal variation in the rotation rate and it could account for a part of the zonal flow pattern. In this work we have adopted a crude representation of smooth part of rotation rate which may not be able to fully represent all the rotation rate variations. We however, do find that if we compute the zonal flow pattern at a region just above the tachocline (around $r = 0.75R_\odot$) the pattern qualitatively matches the zonal flow pattern at a comparable depth, though the errors in both results are too large to see the pattern clearly. As a result, we do not show those results. In addition to the zonal flow pattern, Howe et al. (2000) found an oscillatory pattern with a period of 1.3 yrs in the tachocline region. We do not see any oscillations with a comparable period in the tachocline properties. It should be noted however, that we have not been able to confirm the 1.3 year oscillation (Basu & Antia 2001, 2003; Antia & Basu 2010) even in the zonal flow pattern.

Although we have not examined possible temporal variations in the shape of the convection zone in this work, given that the errors in position of the solar convection-zone base are much smaller, we do not expect the results of Basu & Antia (2001) to be modified by additional data.

4. Conclusions

We have used helioseismic data spanning cycle 23 and beyond to study the properties of the solar tachocline. We confirm that the center of the tachocline is prolate in shape.

The results show unequivocally that the thickness of the tachocline increases with increasing latitude, making the overall shape of the latitude more complex — while the outer boundary is prolate, the inner boundary is close to spherical or perhaps even a little oblate. This appears to be consistent with the fact that the base of the convection zone is almost spherical.

The jump across the tachocline is the only parameter that shows a significant change with solar activity. Other parameters also appear to show some change with time, however the tachocline properties obtained with GONG data and those with MDI do not always show consistent behavior. If the oscillatory temporal variations of tachocline properties are confirmed, it would imply that the solar zonal flow (which is the temporally varying component of solar rotation) penetrates to the base of the convection zone.

This work utilizes data obtained by the Global Oscillation Network Group (GONG) project, managed by the National Solar Observatory, which is operated by AURA, Inc. under a cooperative agreement with the National Science Foundation. The data were acquired by instruments operated by the Big Bear Solar Observatory, High Altitude Observatory, Learmonth Solar Observatory, Udaipur Solar Observatory, Instituto de Astrofísico de Canarias, and Cerro Tololo Inter-American Observatory. This work also utilizes data from the Solar Oscillations Investigation/ Michelson Doppler Imager (SOI/MDI) on the Solar and Heliospheric Observatory (SOHO). SOHO is a project of international cooperation between ESA and NASA. SB acknowledges support from NSF grant ATM 0348837 and NASA grant NXX10AE60G.

REFERENCES

- Antia, H. M., & Basu, S. 2010, *ApJ*, 720, 494
- Antia, H. M., Basu, S., & Chitre, S. M. 1998, *MNRAS*, 298, 543
- Antia, H. M., Basu, S., & Chitre, S. M. 2008a, *ApJ*, 681, 680
- Antia, H. M., Chitre, S. M. & Gough, D. O. 2008b, *A&A*, 477, 657
- Basu, S. 1997, *MNRAS*, 288, 572
- Basu, S., & Antia, H. M. 2001, *MNRAS*, 324, 498
- Basu, S., & Antia, H. M. 2003, *ApJ*, 585, 553
- Brun, A. S., Antia, H. M., Chitre, S. M., Zahn, J.-P. 2002, *A&A*, 391, 725

- Charbonneau, P., Christensen-Dalsgaard, J., Henning, R., Larsen, R. M., Schou, J., Thompson, M. J., Tomczyk, S. 1999, *ApJ*, 527, 445
- Corbard, T., Berthomieu, G., Provost, J., Morel, P. 1998, *A&A*, 330, 1149
- Corbard, T., Blanc-Féraud, L., Berthomieu, G., Provost, J. 1999, *A&A*, 344, 696
- Hill, F., et al. 1996, *Sci.*, 272, 1292
- Howe, R., Christensen-Dalsgaard, J., Hill, F., Komm, R. W., Larsen, R. M., Schou, J., Thompson, M. J., & Toomre, J. 2000, *Science*, 287, 2456
- Howe, R., Rempel, M., Christensen-Dalsgaard, J., Hill, F., Komm, R. W., Schou, J., & Thompson, M. J. 2006, *ApJ*, 634, 1405
- Kosovichev, A. G. 1996, *ApJ*, 469, L61
- Ritzwoller, M. H., & Lively, E. M. 1991, *ApJ*, 369, 557
- Schou, J. 1999, *ApJ*, 523, L181
- Schou, J., et al. 1998, *ApJ*, 505, 390
- Schou, J., et al. 2002, *ApJ*, 567, 1234
- Spiegel, E.A., Zahn, J.-P. 1992, *A&A*, 265, 106
- Vorontsov, S. V., Christensen-Dalsgaard, J., Schou, J., Strakhov, V. N., & Thompson, M. J. 2002, *Sci.*, 296, 101

Table 1: Average properties of the tachocline

Data sets	r_{t1}/R_{\odot}	r_{t3}/R_{\odot}	w_1/R_{\odot}	w_3/R_{\odot}	$\delta\Omega_3$	$\delta\Omega_5$
GONG data sets						
All sets	0.6978 ± 0.0011	0.0033 ± 0.0006	0.0071 ± 0.0005	0.0052 ± 0.0010	-22.28 ± 0.12	-3.52 ± 0.06
$F_{10.7} > 140$ sfu	0.6974 ± 0.0020	0.0029 ± 0.0010	0.0068 ± 0.0009	0.0048 ± 0.0017	-21.76 ± 0.21	-3.34 ± 0.11
$F_{10.7} < 90$ sfu	0.6985 ± 0.0016	0.0036 ± 0.0008	0.0072 ± 0.0007	0.0052 ± 0.0013	-22.66 ± 0.17	-3.61 ± 0.09
cycle 23 min	0.6965 ± 0.0026	0.0040 ± 0.0014	0.0076 ± 0.0012	0.0055 ± 0.0022	-22.75 ± 0.28	-3.37 ± 0.15
cycle 24 min	0.6994 ± 0.0020	0.0033 ± 0.0010	0.0070 ± 0.0009	0.0051 ± 0.0017	-22.62 ± 0.21	-3.74 ± 0.11
MDI data sets						
All sets	0.7021 ± 0.0015	0.0106 ± 0.0007	0.0076 ± 0.0012	0.0086 ± 0.0013	-21.72 ± 0.15	-2.77 ± 0.08
$F_{10.7} > 140$ sfu	0.7029 ± 0.0024	0.0106 ± 0.0012	0.0070 ± 0.0020	0.0072 ± 0.0020	-21.20 ± 0.24	-2.42 ± 0.12
$F_{10.7} < 90$ sfu	0.7026 ± 0.0020	0.0106 ± 0.0010	0.0086 ± 0.0016	0.0086 ± 0.0017	-22.34 ± 0.20	-3.01 ± 0.10
cycle 23 min	0.7002 ± 0.0040	0.0137 ± 0.0019	0.0063 ± 0.0032	0.0112 ± 0.0033	-22.67 ± 0.40	-3.46 ± 0.19
cycle 24 min	0.7034 ± 0.0024	0.0098 ± 0.0012	0.0093 ± 0.0020	0.0079 ± 0.0020	-22.24 ± 0.24	-2.89 ± 0.12

Table 2: Latitudinal variation in the tachocline properties

Lat	GONG data			MDI data		
	r_t/R_{\odot}	w/R_{\odot}	$\delta\Omega$ (nHz)	r_t/R_{\odot}	w/R_{\odot}	$\delta\Omega$ (nHz)
0°	0.6945 ± 0.0013	0.0037 ± 0.0011	18.76 ± 0.45	0.6915 ± 0.0016	0.0028 ± 0.0017	18.95 ± 0.39
15°	0.6956 ± 0.0012	0.0045 ± 0.0008	14.27 ± 0.27	0.6951 ± 0.0016	0.0038 ± 0.0015	14.01 ± 0.37
30°	0.6986 ± 0.0012	0.0084 ± 0.0006	-1.39 ± 0.27	0.7048 ± 0.0015	0.0097 ± 0.0013	-2.14 ± 0.37
45°	0.7027 ± 0.0014	0.0149 ± 0.0015	-30.78 ± 0.32	0.7181 ± 0.0018	0.0204 ± 0.0022	-30.50 ± 0.43
60°	0.7068 ± 0.0017	0.0215 ± 0.0027	-69.40 ± 0.44	0.7313 ± 0.0025	0.0311 ± 0.0036	-66.12 ± 0.57
75°	0.7098 ± 0.0024	0.0264 ± 0.0035	-103.53 ± 0.64	0.7410 ± 0.0030	0.0390 ± 0.0047	-96.80 ± 0.79

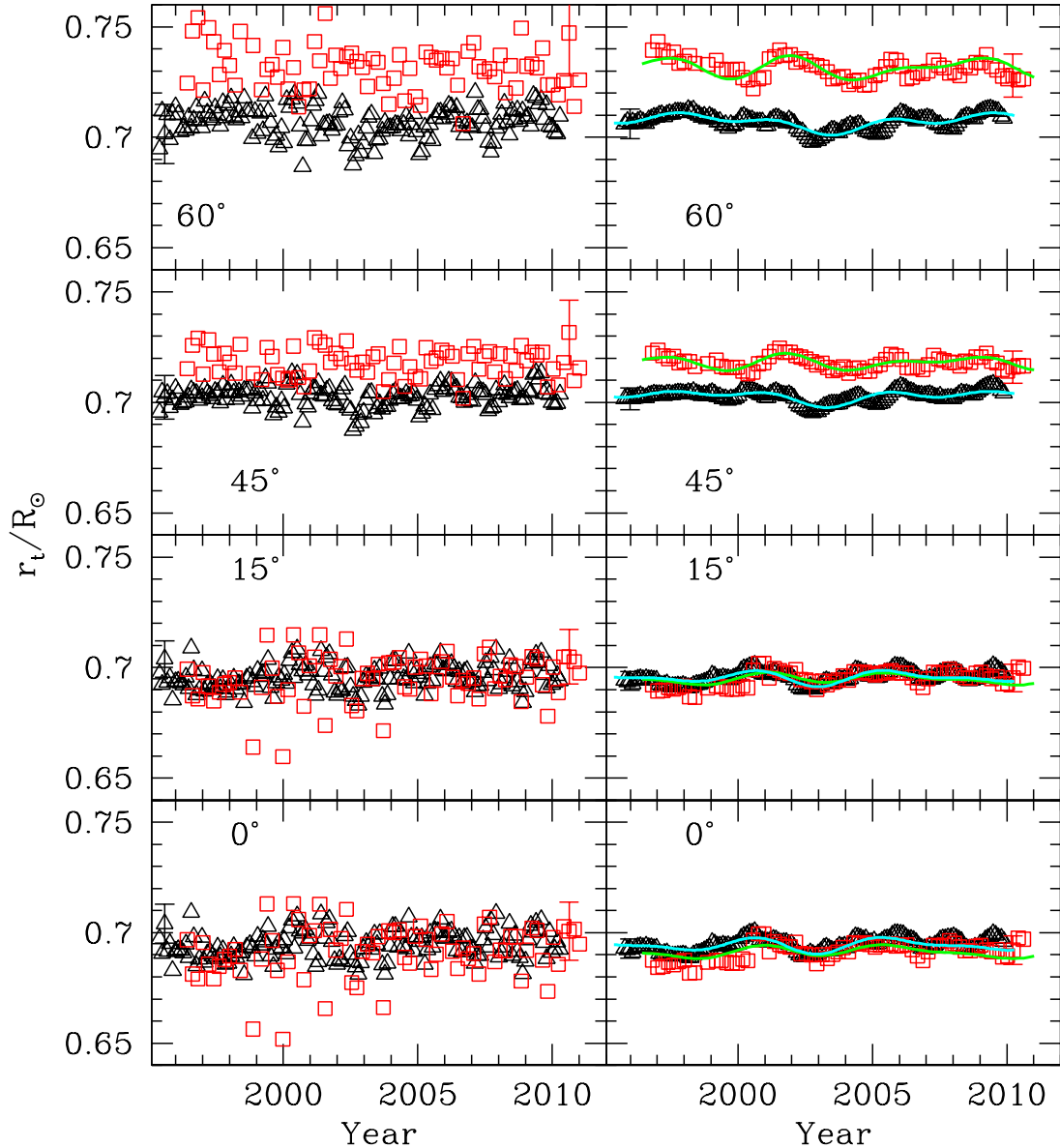


Fig. 1.— The mean position of the tachocline at a few different latitudes plotted as a function of time. The left panels show the results for each data set, while the right panel shows running mean over about a year of data, as well as fits to oscillatory form. The red points are results with MDI data and black are those with GONG data. We show only one representative error-bar each for the GONG and MDI sets for the sake of clarity.

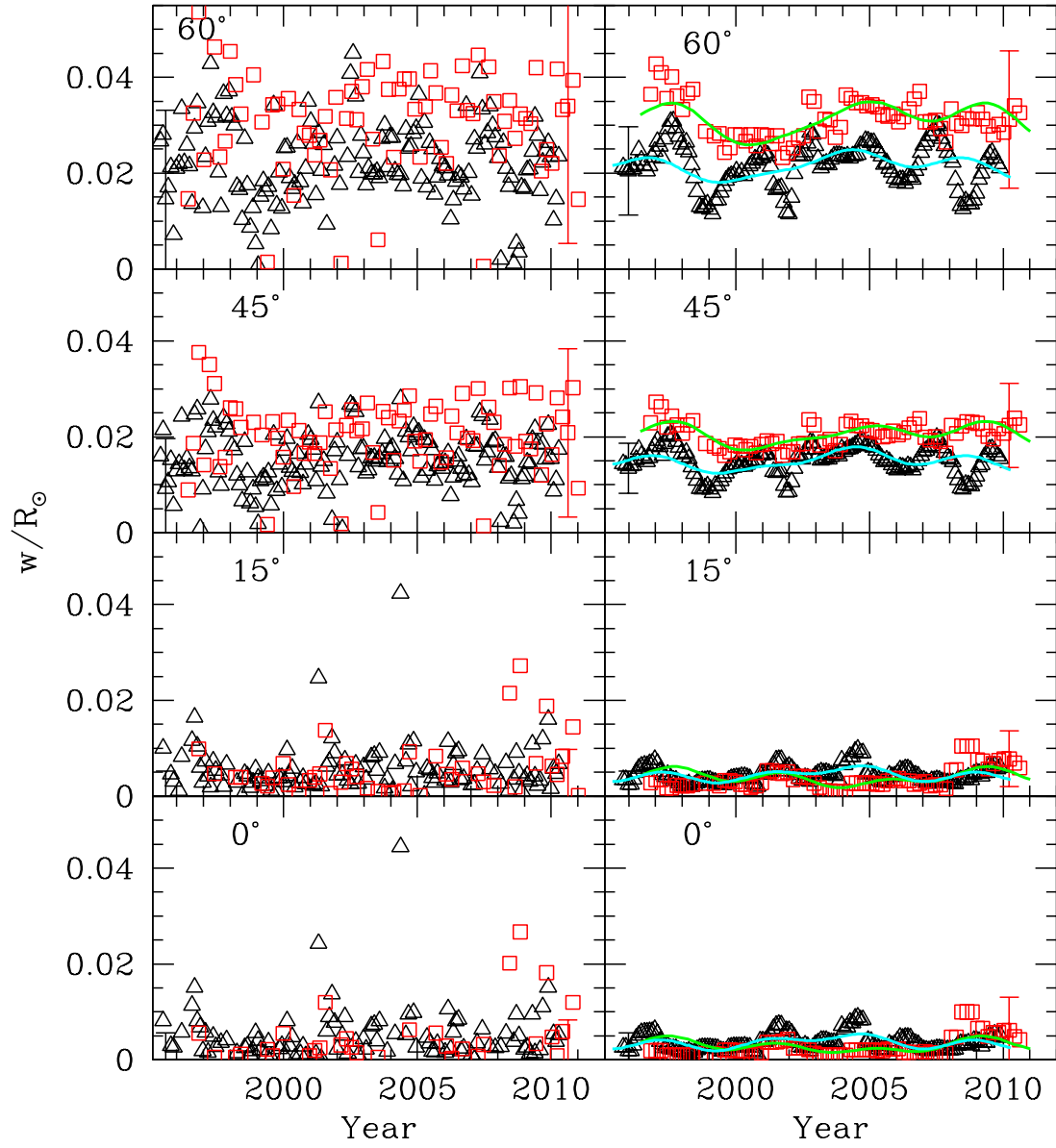


Fig. 2.— Similar to Fig. 1, but showing w , the half-width of the tachocline, instead.

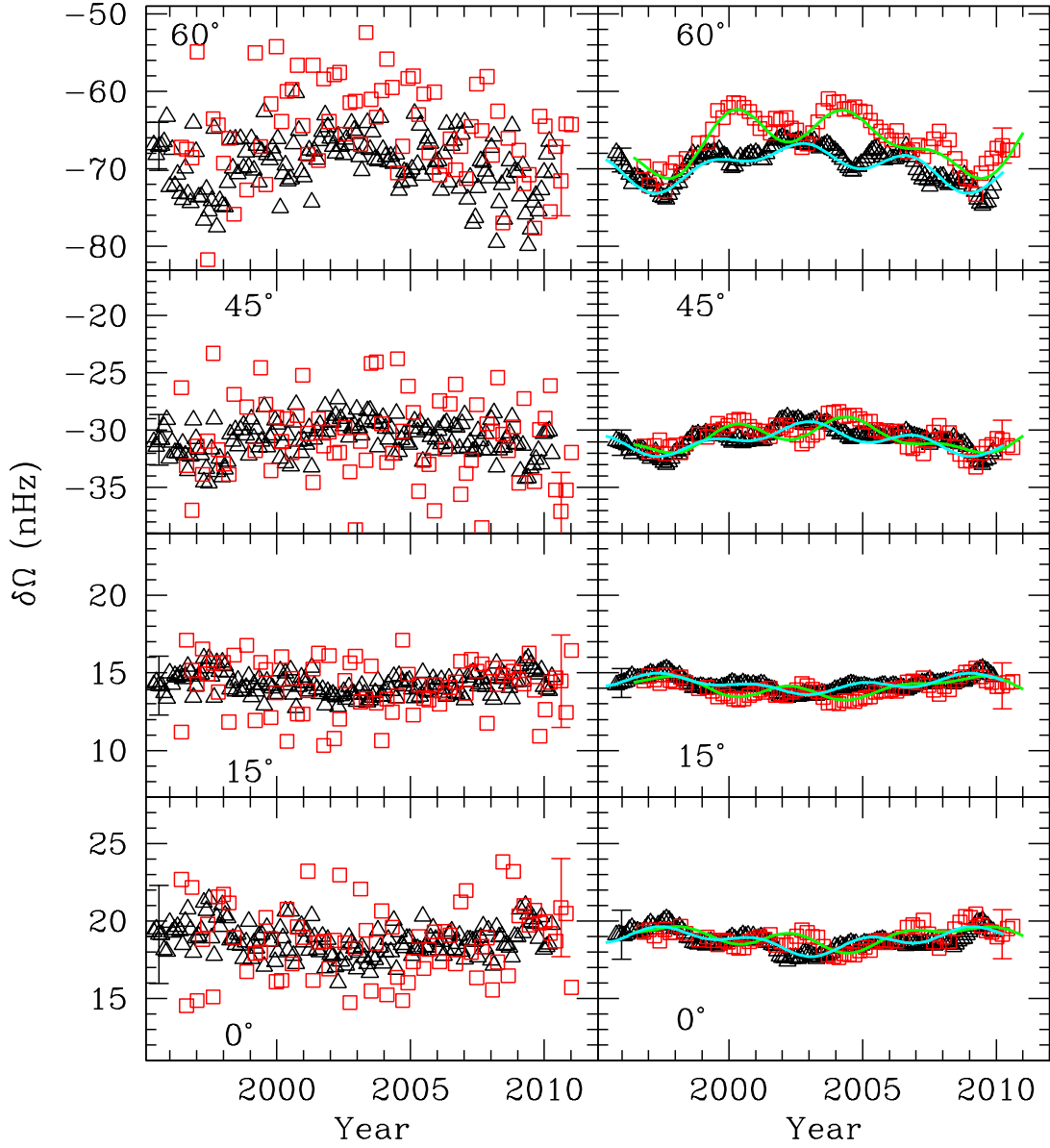


Fig. 3.— Similar to Figs. 1 and 2, but showing $\delta\Omega$, the change in the rotation rate across the tachocline.